

VP-MEL: Visual Prompts Guided Multimodal Entity Linking

Hongze Mi¹, Jinyuan Li², Xuying Zhang¹, Haoran Cheng¹, Jiahao Wang¹, Di Sun³, Gang Pan^{1,2,*}

¹College of Intelligence and Computing, Tianjin University

²School of New Media and Communication, Tianjin University

³Tianjin University of Science and Technology

{mhzqs, jinyuanli, wjhwtt, pangang}@tju.edu.cn

dsun@tust.edu.cn

Abstract

Multimodal Entity Linking (MEL) is extensively utilized in the domains of information retrieval. However, existing MEL methods typically utilize mention words as mentions for retrieval. This results in a significant dependence of MEL on mention words, thereby constraining its capacity to effectively leverage information from both images and text. In situations where mention words are absent, MEL methods struggle to leverage image-text pairs for entity linking. To solve these issues, we introduce a Visual Prompts guided Multimodal Entity Linking (VP-MEL) task. VP-MEL directly marks specific regions within the image. These markers are referred to as visual prompts in VP-MEL. Without mention words, VP-MEL aims to utilize marked image-text pairs to align visual prompts with specific entities in the knowledge bases. A new dataset for the VP-MEL task, VPWiki, is proposed in this paper. Moreover, we propose a framework named FBMEL, which enhances the significance of visual prompts and fully leverages the information in image-text pairs. Experimental results on the VPWiki dataset demonstrate that FBMEL outperforms baseline methods across multiple benchmarks for the VP-MEL task.

1 Introduction

Multimodal entity linking (MEL) (Moon et al., 2018) task aims to utilize both image and text information to disambiguate the mention and link it to the correct entity in the knowledge base(KB). Most MEL works (Gan et al., 2021; Wang et al., 2022a; Dongjie and Huang, 2022; Luo et al., 2023; Zhang et al., 2023a; Xing et al., 2023; Shi et al., 2024) mainly focus on improving the interaction of multimodal information and achieve promising performance. Existing methods represent mentions in the form of mention words and typically assume

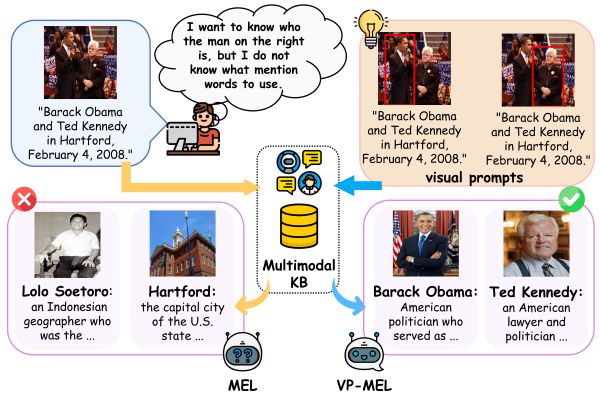


Figure 1: Comparison between MEL and VP-MEL task. In the absence of mention words, MEL faces challenges in performing entity linking for the image content. VP-MEL overcomes this limitation by utilizing visual prompts to link specific regions in the images to the correct entities in knowledge base.

that each mention is associated with a high-quality image, which results in two limitations for MEL.

Text information dependency: MEL relies on selecting mention words for entity linking, which often exhibit significant overlap with entity names in practical applications. This inherent similarity enables mention words to serve as strong cues for identifying specific entities within the knowledge base (KB). Although some ambiguity remains, this overlap substantially simplifies the entity linking task. When mention words are unavailable, MEL struggles to operate effectively and may produce erroneous outputs. As shown in Figure 1, the expected mention is *Ted Kennedy* on the right, but MEL generates incorrect responses, like *Lolo Soetoro* and *Hartford*. Many results, such as *Lolo Soetoro*, are entirely disconnected from both the image and text. Excessive reliance on mention words confines MEL to a text-focused task. It is necessary to introduce a new MEL task to overcome such constraints, enabling MEL to broaden its application

* corresponding authors.

scenarios and adapt to the multimodal era.

Image modality impurity: Compared to text modality, image modality contains more noise. As shown in Figure 1, only the person on the right is relevant, while the one on the left is noise. Incorrect use of image information can significantly impact the results. Most existing coarse-grained methods (Yang et al., 2023; Luo et al., 2023; Wang et al., 2022a) encode the entire image directly, making it difficult to eliminate noise interference. Song et al. (2024) attempts to enhance visual features by utilizing fine-grained image attributes, but it heavily depends on high-quality images and may increase model size and training costs. To utilize images more effectively, it is necessary for MEL to find a way to overcome noise interference in images and focus on the regions related to the mention.

Existing methods demonstrate limited effectiveness in utilizing image information and are overly dependent on mention words as textual cues. In many application scenarios, the inability of users to provide mention words significantly increases the difficulty of MEL. So we ask: *Is it possible to introduce a MEL task that does not depend on mention words, thereby avoiding excessive reliance on text and enhancing the performance of image-based reasoning?*

In this paper, we introduce a new **Visual Prompts guided Multimodal Entity Linking** (VP-MEL) task. As shown in Figure 1, VP-MEL still focuses on addressing the entity linking task for image-text pairs. In the absence of mention words, VP-MEL uses a straightforward method to directly annotate mentions onto images using visual prompts, without any additional complex steps. Free from the constraints of mention words, VP-MEL supports a broader range of applications. It enables effective entity linking even in situations where users are unfamiliar with the textual language or place greater emphasis on image-based information. Moreover, a new VPWiki dataset is constructed based on the existing MEL public datasets, where visual prompts are annotated for each mention within the associated images.

We then propose a **Feature Balanced Multimodal Entity Linking** (FBMEL) framework. Extensive research (Cai et al., 2024; Shtedritski et al., 2023) demonstrates that pre-trained CLIP visual encoders can effectively interpret visual markers. In FBMEL, the CLIP visual encoder is employed to extract both global image features and local features guided by visual prompts. Additionally, a Vision-Language

Model (VLM) equipped with CLIP visual encoder is pre-trained to generate useful text information from visual prompts, serving as an additional supplement to the text information. FBMEL enables visual prompts to deliver both supplementary visual and textual information, ensuring a balanced utilization of image and text while avoiding excessive reliance on a single modality.

Main contributions are summarized as follows:

- (i) We introduce VP-MEL, a new entity linking task that replaces traditional mention words with visual prompts to annotate mentions directly in the images.
- (ii) We construct a high-quality annotated dataset, VPWiki, to enhance the benchmark evaluation of the task. A pipeline is proposed to efficiently automate data annotation for the VP-MEL task.
- (iii) We propose the FBMEL framework to address VP-MEL task by effectively leveraging multimodal information and reducing reliance on a single modality. Compared to prior methods, FBMEL achieves a 20% performance improvement in the VP-MEL task and maintains competitive results in the MEL task.

2 Related Work

2.1 Multimodal Entity Linking

Moon et al. (2018) incorporate images into EL task to address the ambiguity and incompleteness of mentions in social media. Adjali et al. (2020) construct a MEL dataset of social media posts from Twitter and propose a model for jointly learning a representation of both mentions and entities from their textual and visual contexts. Gan et al. (2021) construct a dataset that contains long movie reviews with various related entities and images. Wang et al. (2022c) present a high-quality human-annotated MEL dataset with diversified contextual topics and entity types from Wikinews. In recent years, a multitude of outstanding works in the MEL field (Wang et al., 2022a; Yang et al., 2023; Luo et al., 2023; Shi et al., 2024; Song et al., 2024) have emerged, focusing on the utilization and optimization of multimodal information based on these public datasets. Although multimodal information can enhance entity linking performance, in these methods, text consistently dominates over images.

2.2 Vision Prompt

Region-specific comprehension in complex visual scenes has become a key research topic in the field of Multimodal Computer Vision. Existing methods utilize textual coordinate representations (Zhu et al., 2024; Zhao et al., 2023), learned positional embeddings (Peng et al., 2024; Zhang et al., 2023b; Zhou et al., 2023), or Region of Interest (ROI) features (Zhang et al., 2023b) to anchor language to specific image regions. Cai et al. (2024) propose a user-friendly visual prompting solution that directly overlays visual prompts onto the image canvas in a natural and intuitive way. Inspired by this solution, we introduce visual prompts into MEL to reduce the interference of noise in images and enhance understanding of specific regions.

3 Dataset

To address the VP-MEL task, we construct a VP-Wiki dataset as follows:

Data Collection. Our dataset is built on two benchmark MEL datasets, *i.e.*, WikiDiverse (Wang et al., 2022c) and WikiMEL (Wang et al., 2022a). Appendix A.7 provides detailed information.

Automated Annotation Pipeline. To improve data annotation efficiency, we develop a pipeline that annotates visual prompts in images based on mention words, using the Visual Entailment Module and Visual Grounding Module, inspired by Li et al. (2024). This pipeline can automatically annotate a large amount of high-quality data, significantly reducing the manual annotation workload for subsequent tasks. The details of modules in the pipeline are provided in the Appendix A.6.

Manual Annotation Design. Building on the WikiDiverse and WikiMEL datasets, annotators are provided with an image-text pair and the corresponding mention words. Annotators are required to: 1) annotate relevant visual prompts in the image based on the mention words; 2) remove samples where the image and mention words are unrelated; 3) re-annotate samples with inaccurate pipeline annotations; 4) annotate the entity type for each example (*i.e.*, Person, Organization, Location, Country, Event, Works, Misc).

Manual Annotation Procedure. The annotators include 10 annotators and 2 experienced experts. All annotators have linguistic knowledge and are instructed with detailed annotation principles. Fleiss



Figure 2: An example from VP-MEL and MEL. The red marker in the image represents the visual prompt annotated for the VP-MEL task. The red text indicates the annotated mention words.

	Train	Dev.	Test	Total
pairs	8,000	1,035	1,052	10,087
ment. per pair	1.18	1.16	1.27	1.19
words per pair	9.89	9.80	10.32	9.92

Table 1: Statistics of VPWiki. ment. denotes Mentions.

Kappa score (Fleiss, 1971) of annotators is 0.83, indicating strong agreement among them. We use the Intersection over Union (IoU) metric to assess annotation quality and discard samples with an IoU score below 0.5.

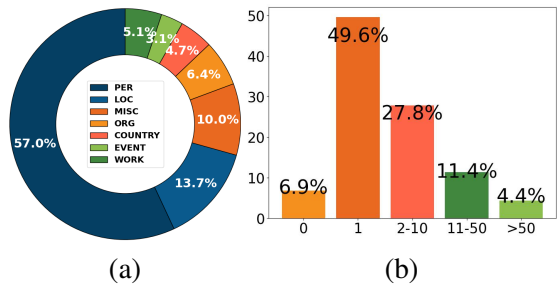


Figure 3: More statistics of VPWiki. (a) Entity type distribution. (b) Distribution of the number of candidate entities per mention.

Dataset Analysis. Figure 2 presents an example from the VP-MEL dataset and compares it with MEL data. In total, 12,720 samples are obtained. After random sampling, the VPWiki dataset is split into training set, validation set, and test set with the ratio of 8:1:1. The detailed data statistics of VPWiki is illustrated in Table 1. The distribution of entity types and the number of candidate entities per mention in the VPWiki dataset are shown in Figure 3. Figure 3(a) uses abbreviations of each entity type for representation. In Figure 3(b), as the number of candidate entities per mention increases, the more difficult the task is.

4 Methodology

In this section, we first formulate the task of VP-MEL, and then go through the details of the proposed **Feature Balanced Multimodal Entity Linking (FBMEL)** framework.

4.1 Task Formulation

Related mathematical notations are defined as follows. The multimodal knowledge base is constructed by a set of entities $\mathcal{E} = \{E_i\}_{i=1}^N$, and each entity is denoted as $E_i = (e_{n_i}, e_{v_i}, e_{d_i}, e_{a_i})$, where the elements of E_i represent entity name, entity images, entity description, and entity attributes, respectively. The mention is denoted as $M_j = (m_{s_j}, m_{v_j})$, where m_{s_j} , m_{v_j} indicate the sentence and the corresponding image. The related entity of mention M_j in the knowledge base is E_i .

The task of VP-MEL targets to retrieve the ground truth entity E_i from the entity set \mathcal{E} of knowledge base based on M_j .

4.2 Visual Encoder

We choose to use pre-trained CLIP visual encoder (Dosovitskiy et al., 2021) to extract image features. The image m_{v_j} of M_j is reshaped into 2D patches, where the number of patches $n = H \times W / P^2$, with $H \times W$ representing the size of the image and P representing the size of each patch. After this, image patches are processed through visual encoder to extract features. The hidden states extracted from m_{v_j} by the CLIP visual encoder are represented as $V_{M_j}^l = [v_{[CLS]}^0; v_{M_j}^1; v_{M_j}^2; \dots; v_{M_j}^n] \in \mathbb{R}^{(n+1) \times d_c}$, where d_c denotes the dimension of the hidden state and l denotes the number of layers in the encoder.

Since CLIP focuses on aligning deep features between images and text and may overlook some low-level visual details (Zhou et al., 2022), we selectively extract features from both the deep and shallow layers of CLIP. Specifically, a shallow feature ($V_{M_j}^3$) is used to represent the textures and geometric shapes in the image, while deep features ($V_{M_j}^{10}, V_{M_j}^{11}, V_{M_j}^{12}$) are used to represent abstract semantic information. We take the hidden states corresponding to the special [CLS] token ($v_{[CLS]}^0 \in \mathbb{R}^{d_c}$) from these layers as the respective visual features F^l . These features are concatenated and normalized using LayerNorm, and then passed through a MLP layer to transform the dimensions to d_v , with the output representing the global features of the image $V_{M_j}^G \in \mathbb{R}^{d_v}$.

$$F^l = v_{[CLS]}^0 \in V_{M_j}^l,$$

$$V_{M_j}^{G'} = \text{LN}(\text{Concat}(F^3, F^{10}, F^{11}, F^{12})) ,$$

$$V_{M_j}^G = \text{MLP}\left(V_{M_j}^{G'}\right).$$

Then, hidden states from the output layer of encoder $V_{M_j}^l$ are passed through a fully connected layer, which also transforms the dimensions to d_v , yielding the local features of the image $V_{M_j}^L \in \mathbb{R}^{(n+1) \times d_v}$:

$$V_{M_j}^L = \text{FC}\left(V_{M_j}^l\right).$$

For the image e_{v_i} of entity E_i , the global feature $V_{E_i}^G$ and local feature $V_{E_i}^L$ are obtained using the same method described above.

4.3 Detective-VLM

To prevent the model from becoming overly dependent on visual information, it is necessary to extract additional textual information to balance contributions of both modalities.

Most VLMs (Liu et al., 2024; Zhu et al., 2024; Ye et al., 2023; Li et al., 2023) choose to use the CLIP visual encoder, which means they have a better ability to focus on the markers in images compared to other visual methods (Cai et al., 2024; Shtedritski et al., 2023). Therefore, we instruction fine-tune a VLM, designed to extract effective information from images. The VLM follows template designed below to further mine potential information from image m_{v_j} and sentence m_{s_j} of mention M_j , assisting in subsequent feature extraction:

Background: $\{Image\}$

Text: $\{Sentence\}$

Question: In the red box of the image, tell me briefly what is the $\{Entity\ Type\}$, and which $\{Entity\ Name\}$ in the text corresponds to the $\{Entity\ Type\}$?

Answer: $\{Entity\ Type\} \{Entity\ Name\}$

We utilize VPWiki dataset to design the fine-tuning dataset, where $\{Image\}$ and $\{Sentence\}$ correspond to m_{v_j} and m_{s_j} in M_j , respectively. During the inference process, $\{Entity\ Name\}$ and $\{Entity\ Type\}$ need to be generated by VLM, where the $\{Entity\ Type\}$ is one of $[Person, Organization, Location, Country, Event, Works, Misc]$. Details of the dataset and model for Detective-VLM can be found in Appendix A.4.

The objective formula for instruction fine-tuning Detective-VLM is expressed as follows:

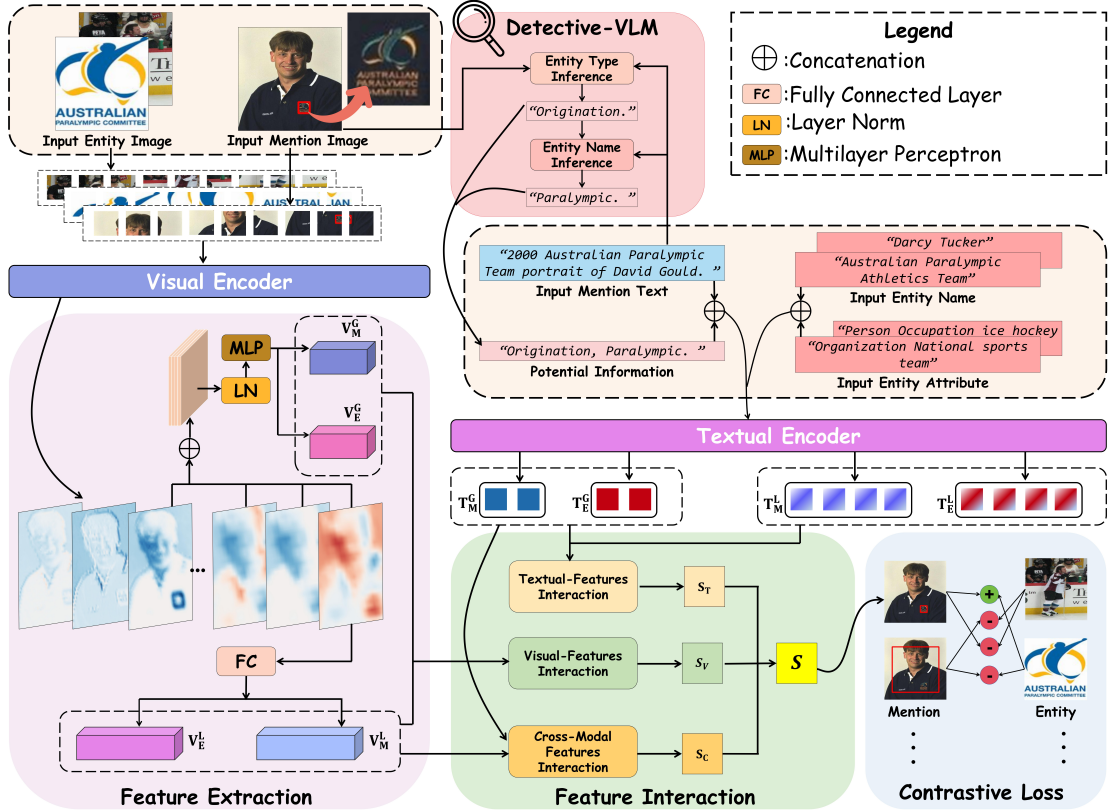


Figure 4: The overall architecture of Feature Balanced Multimodal Entity Linking (FBMEL) framework. The image-text pairs of the Mention and Entity are used together as input. Specifically, Mention Text is the sentence corresponding to Mention Image, while Entity Text consists of Entity Name and Entity Attribute corresponding to the Entity Image in Knowledge Base.

$$\min_{\theta} \sum_{i=1}^N \mathcal{L}(f_{\theta}(x_i), y_i),$$

where f represents the pre-trained VLM, and θ denotes the model parameters. N represents the number of instruction-output pairs, x_i is the i -th instruction, and y_i is the corresponding desired output. \mathcal{L} is defined as:

$$\mathcal{L}(f_{\theta}(x_i), y_i) = - \sum_{t=1}^T \log P_{\theta}(y_i^{(t)} | x_i),$$

where T is the length of output sequence, $y_i(t)$ is the t -th word of the expected output y_i at time step t , and P is conditional probability that the model generates the output $y_i(t)$ at time step t .

Detective-VLM aims to ensure that the output is both accurate and relevant, minimizing the likelihood of generating irrelevant information. Notably, we represent the **Answer** output by VLM as m_{w_j} .

4.4 Textual Encoder

For the mention M_j , after concatenating mention sentence m_{s_j} with m_{w_j} , they form the input se-

quence, with different parts separated by [CLS] and [SEP] tokens:

$$I_{M_j} = [CLS] m_{w_j} [SEP] m_{s_j} [SEP].$$

Hidden states of output layer after the input sequence passes through text encoder are represented as $T_{M_j} = [t_{[CLS]}^0; t_{M_j}^1; \dots; t_{M_j}^{l_t}] \in \mathbb{R}^{(l_t+1) \times d_t}$, where d_t represents the dimension of output layer features, and l_t denotes the length of input. We use the hidden state corresponding to [CLS] as the global feature of the text $T_{M_j}^G \in \mathbb{R}^{d_t}$, and the entire hidden states as the local features of the text $T_{M_j}^L \in \mathbb{R}^{(l_t+1) \times d_t}$.

The input sequence for entity E_i consists of the entity name e_{n_i} and entity attributes e_{a_i} , which can be represented as:

$$I_{E_i} = [CLS] e_{n_i} [SEP] e_{a_i} [SEP].$$

Then, using the above method, we obtain the text features $T_{E_i}^G$ and $T_{E_i}^L$ for the entity.

4.5 Multimodal Feature Interaction

Inspired by the multi-grained multimodal interaction approach (Luo et al., 2023), we build the fea-

ture interaction part. The multimodal feature interaction section consists of three different units. Notably, this section focuses only on introducing the functions of each unit, detailed mathematical derivations are provided in Appendix A.5.

Visual-Features Interaction (VFI). Image features of the mention M_j and the entity E_i interact separately. For feature interaction from M_j to E_i , after passing through VFI:

$$S_V^{M2E} = \text{VFI}_{M2E}(V_{M_j}^G, V_{E_i}^G, V_{E_i}^L).$$

The three input features are sufficiently interacted and integrated, resulting in the similarity matching score S_V^{M2E} . Similarly, for the feature interaction from E_i to M_j , the similarity score S_V^{E2M} can be obtained through VFI:

$$S_V^{E2M} = \text{VFI}_{E2M}(V_{E_i}^G, V_{M_j}^G, V_{M_j}^L).$$

Based on this, the final visual similarity score S_V can be obtained:

$$S_V = (S_V^{M2E} + S_V^{E2M})/2.$$

Textual-Features Interaction (TFI). TFI computes the dot product of the normalized global features $T_{M_j}^G$ and $T_{E_i}^G$, yielding the text global-to-global similarity score S_T^{G2G} :

$$S_T^{G2G} = T_{M_j}^G \cdot T_{E_i}^G.$$

To further uncover fine-grained clues within local features, TFI applies attention mechanism to capture context vector from the local features $T_{M_j}^L$ and $T_{E_i}^L$, producing the global-to-local similarity score S_T^{G2L} between the global feature $T_{E_i}^G$ and the context vector:

$$S_T^{G2L} = \text{TFI}_{G2L}(T_{E_i}^G, T_{M_j}^L, T_{E_i}^L).$$

Based on this, the final textual similarity score S_T can be obtained:

$$S_T = (S_T^{G2G} + S_T^{G2L})/2.$$

Cross-Modal Features Interaction (CMFI). CMFI performs a fine-grained fusion of features across modalities. It integrates visual and textual features to generate a new context vector, h_e :

$$h_e = \text{CMFI}(T_{E_i}^G, V_{E_i}^L).$$

The mention is processed similarly to produce the new context vector h_m :

$$h_m = \text{CMFI}(T_{M_j}^G, V_{M_j}^L).$$

Based on this, the final multimodal similarity score S_C can be obtained:

$$S_C = h_e \cdot h_m.$$

4.6 Contrastive Learning

Based on the three similarity scores S_V , S_T , and S_C , the model is trained using contrastive loss function. For a mention M and entity E , the combined similarity score is the average of the similarity scores from the three independent units:

$$S(M, E) = (S_V + S_T + S_C)/3.$$

This loss function can be formulated as:

$$\mathcal{L}_O = -\log \frac{\exp(S(M_j, E_i))}{\sum_i \exp(S(M_j, E'_i))},$$

where E_i represents the positive entity corresponding to M_j , while E'_i denotes negative entity from the knowledge base \mathcal{E} . It is expected to assign higher evaluation to positive mention-entity pairs and lower evaluation to negative ones.

Similarly, the three independent units are trained separately using contrastive loss function:

$$\mathcal{L}_X = -\log \frac{\exp(S_X(M_j, E_i))}{\sum_i \exp(S_X(M_j, E'_i))}, X \in \{V, T, C\}.$$

The final optimization objective function is expressed as:

$$\mathcal{L} = \mathcal{L}_O + \lambda(\mathcal{L}_V + \mathcal{L}_T + \mathcal{L}_C),$$

where λ is the hyperparameter to control the loss.

5 Experiments

5.1 Experimental Settings

All the training and testing are conducted on a device equipped with 4 Intel(R) Xeon(R) Platinum 8380 CPUs and 8 NVIDIA A800-SXM4-80GB GPUs. Detailed experimental settings are provided in Appendix A.1. In order to conduct a comprehensive assessment of the efficacy of our approach, we compare FBMEL with various competitive MEL baselines and VLM baselines. Detailed introduction of baselines is shown in the Appendix A.2.

Datasets. The VP-MEL experiments are based on VPWiki dataset and MEL experiments are based on the WikiDiverse (Wang et al., 2022c) dataset. Additional experiments and detailed explanations are provided in the Appendix A.8.

5.2 Main Results

Results on VP-MEL. In Table 2a, FBMEL significantly outperforms the other methods. First, among the VLM methods, LLaVA-1.5 is the most competitive, showing differences of 5.14%, 1.97%,

Table 2: Performance comparison on tasks VP-MEL(a) and MEL(b) . Baseline results marked with "*" according to [Sui et al. \(2024\)](#). We run each method three times with different random seeds and report the mean value of every metric. The model marked "†" without VLM. The best score is highlighted in bold. Detailed evaluation metrics are provided in Appendix [A.3](#)

Methods	VP-MEL			Methods	MEL		
	H@1	H@3	H@5		H@1	H@3	H@5
BLIP-2-xl (Li et al., 2023)	15.86	35.41	45.32	ViLT* (Kim et al., 2021)	34.39	51.07	57.83
BLIP-2-xxl (Li et al., 2023)	21.90	37.31	49.70	ALBEF* (Li et al., 2021)	60.59	75.59	83.30
mPLUG-Owl3-7b (Ye et al., 2023)	29.46	30.45	48.94	CLIP* (Radford et al., 2021)	61.21	79.63	85.18
LLaVA-1.5-7b (Liu et al., 2024)	43.20	64.35	65.71	METER* (Dou et al., 2022)	53.14	70.93	77.59
LLaVA-1.5-13b (Liu et al., 2024)	32.93	65.56	66.92	BERT* (Devlin et al., 2019)	55.77	75.73	83.11
MiniGPT-4-7b (Zhu et al., 2024)	28.10	33.53	37.31	BLINK* (Wu et al., 2020)	57.14	78.04	85.32
MiniGPT-4-13b (Zhu et al., 2024)	37.61	37.61	40.03	JMEL* (Adjali et al., 2020)	37.38	54.23	61.00
VELML (Zheng et al., 2022)	22.51	37.61	43.35	VELML (Zheng et al., 2022)	55.53	78.11	84.61
GHMFC (Wang et al., 2022a)	25.53	41.39	48.94	GHMFC (Wang et al., 2022a)	61.17	80.53	86.21
MIMIC (Luo et al., 2023)	24.62	42.35	49.25	MIMIC (Luo et al., 2023)	63.51	81.04	86.43
MELOV (Song et al., 2024)	26.44	42.75	51.51	MELOV* (Sui et al., 2024)	67.32	83.69	87.54
FBMEL(ours)	48.34	67.53	77.50	FBMEL [†] (ours)	63.24	79.76	86.36

(a)

(b)

and 10.58% from FBMEL across the three metrics. Nonetheless, given the substantial data and computational resources required for training LLaVA, our method still demonstrates a clear advantage. Second, the MEL methods exhibit a performance gap compared to our method. MEL methods face challenges in performing effective entity linking when mention words are absent.

Results on MEL. Table 2b presents the experimental comparison results between FBMEL and the MEL baselines. During the training process, the Detective-VLM is removed from FBMEL, and its output is replaced with mention words from WikiDiverse. The metrics of our method are second only to MIMIC and MELOV, with a difference of only 0.27%, 0.28%, and 0.07% compared to MIMIC. FBMEL increases the emphasis on image features while reducing the influence of text features. It is reasonable that FBMEL performs slightly worse than MEL methods in the MEL task. Furthermore, the absence of visual prompts in images somewhat limits the ability of FBMEL to fully utilize visual information.

5.3 Detailed Analysis

Influence of Mention Words on MEL Methods.

As shown in Table 3, without mention words, the performance decreases significantly across three metrics. The average proportion of performance

Methods	WikiDiverse			WikiDiverse*		
	H@1	H@3	H@5	H@1	H@3	H@5
VELML	55.53	78.11	84.61	15.35	26.32	31.38
GHMFC	61.17	80.53	86.21	17.37	28.97	34.36
MIMIC	63.51	81.04	86.43	17.23	29.60	34.84
MELOV	67.32	83.69	87.54	17.66	30.03	36.43
FBMEL [†]	63.24	79.76	86.36	23.87	38.37	45.14

Table 3: Performance comparison of MEL methods in the absence of mention words. The symbol "*" represents the dataset with mention words removed. The model marked "†" without VLM.

drop across three metrics is 72.65%, 64.48%, and 60.28%, respectively. The inability to extract meaningful information from both visual and textual data shows that MEL methods are ill-suited for tasks that lack mention words. We use FBMEL from the VP-MEL task to test on WikiDiverse*. After removing the Detective-VLM, and in the absence of both visual prompts and mention words, FBMEL can still achieve metrics of 23.87%, 38.37%, and 45.14%. This demonstrates that FBMEL in the VP-MEL has a stronger ability to utilize information from both image and text.

Effect Analysis of Detective-VLM. As shown in Table 4, to analyze the effectiveness, we replace the Detective-VLM with various VLMs for experi-

Methods	VP-MEL				
	H@1	H@3	H@5	H@10	H@20
MiniGPT-4-7b	28.55	43.66	52.27	62.99	70.70
MiniGPT-4-13b	27.04	43.96	53.02	63.44	70.72
BLIP-2-xl	37.16	54.38	59.52	66.62	72.81
BLIP-2-xxl	40.63	54.53	61.78	68.73	74.62
LLaVA-1.5-7b	42.45	63.14	69.03	76.74	82.33
LLaVA-1.5-13b	41.54	59.37	66.92	73.11	77.80
Detective-VLM(ours)	48.34	67.53	77.50	82.63	87.92

Table 4: Performance comparison in different VLMs.

V^G -Layer	VP-MEL				
	H@1	H@3	H@5	H@10	H@20
Single Shallow Layer	39.88	60.88	71.00	79.31	86.56
Single Deep Layer	39.73	58.91	69.94	80.82	88.07
(Shallow+Deep) Layers	43.66	60.88	68.58	78.70	84.29
(3 Shallow+Deep) Layers	40.33	59.22	67.37	75.38	83.23
FBMEL	48.34	67.53	77.50	82.63	87.92

Table 5: Comparison of performance across different feature layers in V^G .

ments and obtain the results. Our method achieves the best metrics. Compared with the second best metric, Detective-VLM gains 5.89% absolute improvement of Hit@1. The output of Detective-VLM is concise and effective, allowing it to perform better within FBMEL. Non-fine-tuned VLMs usually generate a large amount of irrelevant information, which interferes with subsequent usage.

Contributions of Visual Features from Different Layers. As shown in Table 5, we combine visual features from different layers during the extraction of V^G to compare the effects of various combinations. In the deeper layers of CLIP visual encoder, the model tends to focus more on abstract, high-level concepts. VP-MEL focuses on aligning high-level concepts between images and text, facilitating the capture of their semantic correspondence. This explains why using a single deep layer feature achieves the highest H@20 score of 88.07%. However, in the VP-MEL task, low-level texture details are equally important. Shallow texture features need to be extracted to help the model focus on the presence of visual prompts. Based on this, we choose to concatenate the deep features with the shallow features. Experimental results show that the best performance is achieved when the

Methods	VP-MEL				
	H@1	H@3	H@5	H@10	H@20
FBMEL	48.34	67.53	77.50	82.63	87.92
FBMEL [†]	35.65	53.93	65.26	73.57	80.51
FBMEL [*]	35.03	53.80	65.01	73.26	80.39

Table 6: The model marked "†" without VLM. The model marked "*" without VLM and Visual Prompts.

proportion of deep features is larger.

Ablation Study. In Table 6, we conduct ablation study of FBMEL framework. First, the Detective-VLM is removed from FBMEL. All metrics exhibit a downward trend. Even without additional textual information, FBMEL can still effectively perform entity linking. Moreover, without the Detective-VLM, FBMEL still outperforms MEL methods. This indicates that FBMEL is capable of leveraging information from both images and text more efficiently than MEL methods. To further evaluate the contribution of Visual Prompts, we removed the visual prompts from the images based on the previous setup. All metrics show decreases. This indicates that visual prompts help the model focus on specific regions in images. The function of visual prompts is significantly enhanced by the Detective-VLM, which facilitates the ability to derive more comprehensive information from images.

6 Conclusion

In this paper, we introduce a new task VP-MEL and construct a new dataset VPWiki, aiming to utilize visual prompts to broaden application scenarios of MEL. To address the VP-MEL task, we propose FBMEL, a method designed to effectively leverage visual prompts for extracting meaningful information from image-text data. Extensive experimental results demonstrate that FBMEL surpasses state-of-the-art methods, effectively reducing dependency on textual information while significantly improving the utilization of visual information. VP-MEL significantly reduces the constraints of mention words and expands the applicability of MEL to real-world scenarios.

Limitations

VP-MEL expands the application scenarios of MEL, allowing users to directly annotate areas of interest within images. However, this requires

the image and text to be correlated to some extent. When the image and text are not correlated, the performance of VP-MEL can be limited. We choose to use grounding box as the format for visual prompts. In real-world application scenarios, users may use any irregular shape to make markings. In future work, the design of visual prompts will be enhanced. We hope this work can encourage more research to apply the recent advanced techniques from both natural language processing and computer vision fields to improve its performance.

Ethics Statement

The datasets employed in this paper, WikiDiverse, WikiMEL, and RichpediaMEL, are all publicly accessible. As such, the images, texts, and knowledge bases referenced in this study do not infringe upon the privacy rights of any individual.

References

Omar Adjali, Romaric Besançon, Olivier Ferret, Hervé Le Borgne, and Brigitte Grau. 2020. Multimodal entity linking for tweets. In *ECIR*, pages 463–478. Springer.

Mu Cai, Haotian Liu, Siva Karthik Mustikovela, Gregory P. Meyer, Yuning Chai, Dennis Park, and Yong Jae Lee. 2024. *Vip-llava: Making large multimodal models understand arbitrary visual prompts*. In *CVPR*, pages 12914–12923.

Jacob Devlin, Ming-Wei Chang, Kenton Lee, and Kristina Toutanova. 2019. *BERT: Pre-training of deep bidirectional transformers for language understanding*. In *HLT-NAACL*, pages 4171–4186, Minneapolis, Minnesota. Association for Computational Linguistics.

Zhang Dongjie and Longtao Huang. 2022. *Multimodal knowledge learning for named entity disambiguation*. In *Findings of ACL: EMNLP*, pages 3160–3169, Abu Dhabi, United Arab Emirates. Association for Computational Linguistics.

Alexey Dosovitskiy, Lucas Beyer, Alexander Kolesnikov, Dirk Weissenborn, Xiaohua Zhai, Thomas Unterthiner, Mostafa Dehghani, Matthias Minderer, Georg Heigold, Sylvain Gelly, Jakob Uszkoreit, and Neil Houlsby. 2021. *An image is worth 16x16 words: Transformers for image recognition at scale*. In *ICLR*. OpenReview.net.

Zi-Yi Dou, Yichong Xu, Zhe Gan, Jianfeng Wang, Shuohang Wang, Lijuan Wang, Chenguang Zhu, Pengchuan Zhang, Lu Yuan, Nanyun Peng, et al. 2022. An empirical study of training end-to-end vision-and-language transformers. In *CVPR*, pages 18166–18176.

Joseph L Fleiss. 1971. Measuring nominal scale agreement among many raters. In *Psychological bulletin*, volume 76, page 378. American Psychological Association.

Jingru Gan, Jinchang Luo, Haiwei Wang, Shuhui Wang, Wei He, and Qingming Huang. 2021. *Multimodal entity linking: A new dataset and a baseline*. In *ACM Multimedia*, page 993–1001, New York, NY, USA. Association for Computing Machinery.

Wonjae Kim, Bokyung Son, and Ildoo Kim. 2021. *Vilt: Vision-and-language transformer without convolution or region supervision*. In *ICML*, volume 139 of *Proceedings of Machine Learning Research*, pages 5583–5594. PMLR.

Jinyuan Li, Han Li, Di Sun, Jiahao Wang, Wenkun Zhang, Zan Wang, and Gang Pan. 2024. *LLMs as bridges: Reformulating grounded multimodal named entity recognition*. In *Findings of ACL: ACL*, pages 1302–1318, Bangkok, Thailand. Association for Computational Linguistics.

Junnan Li, Dongxu Li, Silvio Savarese, and Steven Hoi. 2023. *BLIP-2: Bootstrapping language-image pre-training with frozen image encoders and large language models*. In *ICML*, volume 202 of *Proceedings of Machine Learning Research*, pages 19730–19742. PMLR.

Junnan Li, Ramprasaath Selvaraju, Akhilesh Gotmare, Shafiq Joty, Caiming Xiong, and Steven Chu Hong Hoi. 2021. Align before fuse: Vision and language representation learning with momentum distillation. In *NeurIPS*, volume 34, pages 9694–9705.

Haotian Liu, Chunyuan Li, Yuheng Li, and Yong Jae Lee. 2024. Improved baselines with visual instruction tuning. In *CVPR*, pages 26296–26306.

Pengfei Luo, Tong Xu, Shiwei Wu, Chen Zhu, Linli Xu, and Enhong Chen. 2023. *Multi-grained multimodal interaction network for entity linking*. In *KDD*, page 1583–1594, New York, NY, USA. Association for Computing Machinery.

Seungwhan Moon, Leonardo Neves, and Vitor Carvalho. 2018. *Multimodal named entity disambiguation for noisy social media posts*. In *ACL (Volume 1: Long Papers)*, pages 2000–2008, Melbourne, Australia. Association for Computational Linguistics.

Zhiliang Peng, Wenhui Wang, Li Dong, Yaru Hao, Shao-han Huang, Shuming Ma, Qixiang Ye, and Furu Wei. 2024. *Grounding multimodal large language models to the world*. In *ICLR*. OpenReview.net.

Alec Radford, Jong Wook Kim, Chris Hallacy, Aditya Ramesh, Gabriel Goh, Sandhini Agarwal, Girish Sastry, Amanda Askell, Pamela Mishkin, Jack Clark, et al. 2021. Learning transferable visual models from natural language supervision. In *ICML*, pages 8748–8763. PMLR.

Senbao Shi, Zhenran Xu, Baotian Hu, and Min Zhang. 2024. [Generative multimodal entity linking](#). In *LREC-COLING*, pages 7654–7665, Torino, Italia. ELRA and ICCL.

Aleksandar Shtedritski, Christian Rupprecht, and Andrea Vedaldi. 2023. What does clip know about a red circle? visual prompt engineering for vlms. In *ICCV*, pages 11987–11997.

Shezheng Song, Shan Zhao, Chengyu Wang, Tianwei Yan, Shasha Li, Xiaoguang Mao, and Meng Wang. 2024. [A dual-way enhanced framework from text matching point of view for multimodal entity linking](#). In *AAAI*, volume 38, pages 19008–19016.

Xuhui Sui, Ying Zhang, Yu Zhao, Kehui Song, Baohang Zhou, and Xiaojie Yuan. 2024. [MELOV: Multimodal entity linking with optimized visual features in latent space](#). In *Findings of ACL: ACL*, pages 816–826, Bangkok, Thailand. Association for Computational Linguistics.

Peng Wang, Jiangheng Wu, and Xiaohang Chen. 2022a. [Multimodal entity linking with gated hierarchical fusion and contrastive training](#). In *SIGIR*, page 938–948, New York, NY, USA. Association for Computing Machinery.

Peng Wang, An Yang, Rui Men, Junyang Lin, Shuai Bai, Zhikang Li, Jianxin Ma, Chang Zhou, Jingren Zhou, and Hongxia Yang. 2022b. [Ofa: Unifying architectures, tasks, and modalities through a simple sequence-to-sequence learning framework](#). In *ICML*, pages 23318–23340. PMLR.

Xuwu Wang, Junfeng Tian, Min Gui, Zhixu Li, Rui Wang, Ming Yan, Lihan Chen, and Yanghua Xiao. 2022c. [WikiDiverse: A multimodal entity linking dataset with diversified contextual topics and entity types](#). In *ACL (Volume 1: Long Papers)*, pages 4785–4797, Dublin, Ireland. Association for Computational Linguistics.

Ledell Wu, Fabio Petroni, Martin Josifoski, Sebastian Riedel, and Luke Zettlemoyer. 2020. [Scalable zero-shot entity linking with dense entity retrieval](#). In *EMNLP*, pages 6397–6407, Online. Association for Computational Linguistics.

Shangyu Xing, Fei Zhao, Zhen Wu, Chunhui Li, Jianbing Zhang, and Xinyu Dai. 2023. [Drin: Dynamic relation interactive network for multimodal entity linking](#). In *ACM Multimedia*, page 3599–3608, New York, NY, USA. Association for Computing Machinery.

Chengmei Yang, Bowei He, Yimeng Wu, Chao Xing, Lianghua He, and Chen Ma. 2023. [MMEL: A joint learning framework for multi-mention entity linking](#). In *UAI*, volume 216 of *Proceedings of Machine Learning Research*, pages 2411–2421. PMLR.

Qinghao Ye, Haiyang Xu, Guohai Xu, Jiabo Ye, Ming Yan, Yiyang Zhou, Junyang Wang, Anwen Hu, Pengcheng Shi, Yaya Shi, et al. 2023. [mplug-owl: Modularization empowers large language models with multimodality](#). *arXiv preprint arXiv:2304.14178*.

Qinghao Ye, Haiyang Xu, Jiabo Ye, Ming Yan, Anwen Hu, Haowei Liu, Qi Qian, Ji Zhang, and Fei Huang. 2024. [mplug-owl2: Revolutionizing multi-modal large language model with modality collaboration](#). In *CVPR*, pages 13040–13051.

Gongrui Zhang, Chenghuan Jiang, Zhongheng Guan, and Peng Wang. 2023a. [Multimodal entity linking with mixed fusion mechanism](#). In *DASFAA*, pages 607–622. Springer.

Shilong Zhang, Peize Sun, Shoufa Chen, Min Xiao, Wenqi Shao, Wenwei Zhang, Kai Chen, and Ping Luo. 2023b. [Gpt4roi: Instruction tuning large language model on region-of-interest](#). *arXiv preprint arXiv:2307.03601*.

Liang Zhao, En Yu, Zheng Ge, Jinrong Yang, Haoran Wei, Hongyu Zhou, Jianjian Sun, Yuang Peng, Runpei Dong, Chunrui Han, et al. 2023. [Chatspot: Bootstrapping multimodal llms via precise referring instruction tuning](#). *arXiv preprint arXiv:2307.09474*.

Qiushuo Zheng, Hao Wen, Meng Wang, and Guilin Qi. 2022. [Visual entity linking via multi-modal learning](#). In *Data Intel*, volume 4, pages 1–19.

Chong Zhou, Chen Change Loy, and Bo Dai. 2022. [Extract free dense labels from clip](#). In *ECCV*, pages 696–712. Springer.

Qiang Zhou, Chaozhi Yu, Shaofeng Zhang, Sitong Wu, Zhibing Wang, and Fan Wang. 2023. [Regionclip: A unified multi-modal pre-training framework for holistic and regional comprehension](#). *arXiv preprint arXiv:2308.02299*.

Deyao Zhu, Jun Chen, Xiaoqian Shen, Xiang Li, and Mohamed Elhoseiny. 2024. [MiniGPT-4: Enhancing vision-language understanding with advanced large language models](#). In *ICLR*. OpenReview.net.

A Appendix

A.1 Experimental Settings

For our proposed model framework, we use pre-trained ViT-B/32 (Dosovitskiy et al., 2021) as the visual encoder, initialized with weights from CLIP-ViT-Base-Patch32¹, with d_v and d_c set to 96. The batch size is set to 128. For the text encoder, we select pre-trained BERT model (Devlin et al., 2019), setting the maximum input length for text to 40 and the output feature dimension d_t to 512. We train and test on a device equipped with 4 Intel(R) Xeon(R) Platinum 8380 CPUs and 8 NVIDIA A800-SXM4-80GB GPUs.

¹<https://huggingface.co/openai/clip-vit-base-patch32>

A.2 Descriptions of Baselines

To thoroughly evaluate the performance of our method, we compare it against strong MEL baselines, including **BERT** (Devlin et al., 2019), **BLINK** (Wu et al., 2020), **JMEL** (Adjali et al., 2020), **VELML** (Zheng et al., 2022), **GHMFC** (Wang et al., 2022a), **MIMIC** (Luo et al., 2023) and **MELOV** (Sui et al., 2024).

Additionally, we select robust VLMs for comparison, including **BLIP-2-xl**², **BLIP-2-xxl**³ (Li et al., 2023), **mPLUG-Owl3-7b**⁴ (Ye et al., 2023), **LLaVA-1.5-7b**⁵, **LLaVA-1.5-13b**⁶ (Liu et al., 2024), **MiniGPT-4-7b**⁷, **MiniGPT-4-13b**⁸ (Zhu et al., 2024), **ViLT** (Kim et al., 2021), **ALBEF** (Li et al., 2021), **CLIP** (Radford et al., 2021), and **METER** (Dou et al., 2022). we reimplemented JMEL, VELML and MELOV according to the original literature due to they did not release the code. We ran the official implementations of the other baselines with their default settings.

- **BERT** (Devlin et al., 2019) is a pre-trained language model based on the Transformer architecture, designed to deeply model contextual information from both directions of a text, generating general-purpose word representations.
- **BLINK** (Wu et al., 2020) present a two-stage zero-shot linking algorithm, where each entity is defined only by a short textual description.
- **JMEL** (Adjali et al., 2020) extracts both unigram and bigram embeddings as textual features. Different features are fused by concatenation and a fully connected layer.
- **VELML** (Zheng et al., 2022) utilizes VGG-16 network to obtain object-level visual features. The two modalities are fused with additional attention mechanism.
- **GHMFC** (Wang et al., 2022a) extracts hierarchical features of text and visual co-attention through

the multi-modal co-attention mechanism.

- **MIMIC** (Luo et al., 2023) devise three interaction units to sufficiently explore and extract diverse multimodal interactions and patterns for entity linking.
- **MELOV** (Sui et al., 2024) incorporates inter-modality generation and intra-modality aggregation.
- **BLIP-2** (Li et al., 2023) effectively utilizes the noisy web data by bootstrapping the captions, where a captioner generates synthetic captions and a filter removes the noisy ones.
- **mPLUG-Owl3** (Ye et al., 2023) propose novel hyper attention blocks to efficiently integrate vision and language into a common language-guided semantic space, thereby facilitating the processing of extended multi-image scenarios.
- **LLaVA-1.5** (Liu et al., 2024) is an end-to-end trained large multimodal model that connects a vision encoder and an LLM for general purpose visual and language understanding.
- **MiniGPT-4** (Zhu et al., 2024) aligns a frozen visual encoder with a frozen LLM, Vicuna, using just one projection layer.
- **ViLT** (Kim et al., 2021) commissions the transformer module to extract and process visual features in place of a separate deep visual embedder.
- **ALBEF** (Li et al., 2021) introduce a contrastive loss to align the image and text representations before fusing them through cross-modal attention, which enables more grounded vision and language representation learning.
- **CLIP** (Radford et al., 2021) is a neural network trained on a variety of (image, text) pairs. It can be instructed in natural language to predict the most relevant text snippet, given an image.
- **METER** (Dou et al., 2022) systematically investigate how to train a fully-transformer VLP model in an end-to-end manner.

A.3 Evaluation Metrics

For evaluation, we utilize Top-k accuracy as the metric that can be calculated by the following formula:

$$\text{Accuracy}_{top-k} = \frac{1}{N} \sum_i^N I(t_i \in y_i^k)$$

where N represents the total number of samples, and I is the indicator function. When the receiving condition is satisfied, I is set to 1, and 0 otherwise.

²<https://huggingface.co/Salesforce/blip2-flan-t5-xl-coco>
³<https://huggingface.co/Salesforce/blip2-flan-t5-xxl>
⁴<https://huggingface.co/mPLUG/mPLUG-Owl3-7B-240728>
⁵<https://huggingface.co/liuhaotian/llava-v1.5-7b>
⁶<https://huggingface.co/liuhaotian/llava-v1.5-13b>
⁷<https://drive.google.com/file/d/1RY9jV0dyqLX-o38LrumkRh6Jtaop58R/view?usp=sharing>
⁸https://drive.google.com/file/d/1a4zLvaIDBr-36pasffmgpvH5P7CKmpze/view?usp=share_link

A.4 Detective-VLM

Detective-VLM is based on mplug-owl2 (Ye et al., 2024), and we perform instruction fine-tuning on mplug-owl2-llama2-7b⁹.

We utilize VPWiki dataset to design the fine-tuning dataset, where $\{\text{Image}\}$ and $\{\text{Sentence}\}$ correspond to m_{v_j} and m_{s_j} in M_j , respectively. In the fine-tuning dataset, the $\{\text{Entity Name}\}$ corresponds to the mention words in M_j that are associated with the Visual prompt, the $\{\text{Entity Type}\}$ is one of $[\text{Person}, \text{Organization}, \text{Location}, \text{Country}, \text{Event}, \text{Works}, \text{Misc}]$.

A.5 Feature Interaction Formula

Visual-Features Interaction (VFI). The two similarity scores S_V^{M2E} and S_V^{E2M} in visual feature interaction are calculated using the same method. Here, we take S_V^{M2E} as an example.

$$\begin{aligned} \bar{h}_p &= \text{MeanPooling}(V_{E_i}^L), \\ h_{vc} &= \text{FC}(\text{LayerNorm}(\bar{h}_p + V_{M_j}^G)), \\ h_{vg} &= \text{Tanh}(\text{FC}(h_{vc})), \\ h_v &= \text{LayerNorm}(h_{vg} * h_{vc} + V_{E_i}^G), \\ S_V^{M2E} &= h_v \cdot V_{M_j}^G. \end{aligned}$$

Textual-Features Interaction (TFI). The calculation of the global-to-local similarity score S_T^{G2L} incorporates an attention mechanism as follows:

$$Q, K, V = T_{E_i}^L W_{tq}, T_{M_j}^L W_{tk}, T_{M_j}^L W_{tv},$$

$$H_t = \text{softmax}\left(\frac{QK^T}{\sqrt{d_T}}\right)V,$$

where $T_{E_i}^L W_{tq}$, $T_{M_j}^L W_{tk}$, $T_{M_j}^L W_{tv}$ are learnable matrices.

$$h_t = \text{LayerNorm}(\text{MeanPooling}(H_t)),$$

$$S_T^{G2L} = \text{FC}(T_{E_i}^G) \cdot h_t.$$

Cross-Modal Features Interaction (CMFI). CMFI performs alignment and fusion of features from different modalities.

$$h_{et}, h_{mt} = \text{FC}_{c1}(T_{E_i}^G), \text{FC}_{c1}(T_{M_j}^G),$$

$$H_{ev}, H_{mv} = \text{FC}_{c2}(V_{E_i}^L), \text{FC}_{c2}(V_{M_j}^L),$$

⁹<https://huggingface.co/MAGAer13/mplug-owl2-llama2-7b>

	WIKIDiverse	WikiMEL
Sentences	7,405	22,070
M. in train	11,351	18,092
M. in valid	1,664	2,585
M. in test	2,078	5,169
Entities	132,460	109,976

Table 7: Statistics of WIKIDiverse and WikiMEL. M. denotes Mentions.

in which FC_{c1} is defined by $W_{c1} \in \mathbb{R}^{d_t \times d_c}$ and $b_{c1} \in \mathbb{R}^{d_c}$, FC_{c2} is defined by $W_{c2} \in \mathbb{R}^{d_v \times d_c}$ and $b_{c2} \in \mathbb{R}^{d_c}$.

$$\alpha_i = \frac{\exp(h_{et} \cdot H_{ev}^i)}{\sum_1^{n+1} \exp(h_{et} \cdot H_{ev}^i)},$$

$$h_{ec} = \sum_i^n \alpha_i * H_{ev}^i, i \in [1, 2, \dots, (n+1)],$$

$$h_{eg} = \text{Tanh}(\text{FC}_{c3}(h_{et})),$$

in which FC_{c3} is defined by $W_{c3} \in \mathbb{R}^{d_c \times d_c}$ and $b_{c3} \in \mathbb{R}^{d_c}$.

$$h_e = \text{LayerNorm}(h_{eg} * h_{et} + h_{ec}).$$

By replacing inputs h_{et} and H_{ev} with h_{mt} and H_{mv} , h_m can be obtained using the aforementioned formula.

A.6 Pipeline Module Settings

The construction of the pipeline based on the Visual Entailment Module and Visual Grounding Module is inspired by Li et al. (2024). In the pipeline, Visual Entailment Module is employed to evaluate the relationship between the mention words and the corresponding images. After filtering out the highly relevant data, Visual Grounding Module annotates the grounding box in the images. For the Visual Entailment Module and Visual Grounding Module, we choose OFA_{large(VE)} and OFA_{large(VG)} (Wang et al., 2022b), respectively.

A.7 WikiDiverse and WikiMEL

WikiDiverse is a high-quality human-annotated MEL dataset with diversified contextual topics and entity types from Wikinews, which uses Wikipedia as the corresponding knowledge base. WikiMEL is collected from Wikipedia entities pages and contains more than 22k multimodal sentences. The statistics of WIKIDiverse and WikiMEL are shown

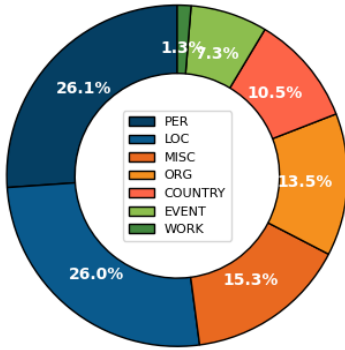


Figure 5: Entity type distribution of WIKIDiverse.

Methods	WikiMEL			RichpediaMEL		
	H@1	H@3	H@5	H@1	H@3	H@5
ViLT*	72.64	84.51	87.86	45.85	62.96	69.80
ALBEF*	78.64	88.93	91.75	65.17	82.84	88.28
CLIP*	83.23	92.10	94.51	67.78	85.22	90.04
METER*	72.46	84.41	88.17	63.96	82.24	87.08
BERT*	74.82	86.79	90.47	59.55	81.12	87.16
BLINK*	74.66	86.63	90.57	58.47	81.51	88.09
JMEL*	64.65	79.99	84.34	48.82	66.77	73.99
VELML	68.90	83.50	87.77	62.80	82.04	87.84
GHMFC	75.54	88.82	92.59	76.95	88.85	92.11
FBMEL [†]	81.15	92.38	93.44	78.96	91.63	94.36
MIMIC	87.98	95.07	96.37	81.02	91.77	94.38
MELOV*	88.91	95.61	96.58	84.14	92.81	94.89

Table 8: Baseline results marked with "*" according to [Sui et al. \(2024\)](#). We run each method three times with different random seeds and report the mean value of every metric. The model marked '[†]' is the FBMEL retrained on the WikiMEL and RichpediaMEL datasets individually. The best score is highlighted in bold.

in Table 7. The entity type distribution of WIKIDiverse is illustrated in Figure 5.

During the data collection process, we selected all of the WIKIDiverse data and 5,000 samples from the WikiMEL dataset. Compared to WikiMEL, the images in the WIKIDiverse dataset are more content-rich and more representative of real-world application scenarios, making them better suited to the needs of the VP-MEL task in practical applications. Therefore, WIKIDiverse constitutes a larger portion of the VPWiki dataset. We integrate the KB from both datasets. The entity set consists of all the entities in the main namespace with the size of 28M.

A.8 Additional Experiments and Experimental Descriptions

The knowledge base (KB) used in the WikiMEL and RichpediaMEL datasets differs from that of VPWiki and WIKIDiverse. To thoroughly evaluate the performance of the FBMEL framework in the MEL task, we retrained FBMEL on the WikiMEL and RichpediaMEL datasets. Notably, during the retraining process, neither visual prompts nor the Detective-VLM are used, meaning that in this experiment, FBMEL can only be regarded as a MEL model. The experimental results are shown in Table 8. FBMEL is second only to MIMIC and MELOV, demonstrating its competitive performance as an MEL method.

A.9 Case Study

To clearly demonstrate the proposed VP-MEL task and the FBMEL model, we present case studies and compare them against two strong competitors (*i.e.*, LLaVA-1.5 and MIMIC), in Figure 6. As shown in Figure 6a, in the first case, all three methods correctly predicted the entity. FBMEL makes full use of both image and text information, allowing it to more effectively distinguish between the different individuals in the image. LLaVA-1.5 may be overwhelmed by the textual information, while MIMIC struggles to identify the correct entity when the mention words are unavailable. In the second case, both LLaVA-1.5 and MIMIC retrieve Endeavour as the first choice. Only FBMEL, with the guidance of Visual Prompts and integration of textual information, correctly identified the right entity. In Figure 6b, we present the error cases. In the first case, when the content of the image interferes with the visual prompt, it impairs FBMEL's reasoning process. The red box in the image bears a high similarity to the visual prompt. As a result, FBMEL incorrectly focuses on the wrong region of the image, ranking *Donald Trump* first. When FBMEL encounters difficulties in distinguishing the objects within the image's visual prompts, it leads to incorrect inferences. For example, in the second case, the distinguishing features of the two individuals in the image are obstructed, causing FBMEL to encounter difficulties in differentiating between the two. The image content in real-world data is often complex, making VP-MEL a task that presents significant challenges. We hope that this task can be further refined and developed over time.

Input	Ground Truth Entity	VP-MEL (FBMEL)	LLaVA-1.5	MEL (MIMIC)
 Cosplayers cosplaying Marvel Cinematic Universe's Iron Man (left) and Spider-Man (right).	Q79037 Spider-Man fictional character in Marvel Comics	TOP-1  Q79037 Spider-Man  TOP-2  Q4508517 Spider-Man in other media TOP-3  Q79037 Iron Man's armor	TOP-1  Q79037 Iron Man's armor  TOP-2  Q79037 Spider-Man  TOP-3  Q642878 Marvel Cinematic Universe	TOP-1  Q79037 Iron Man's armor  TOP-2  Q4508517 Spider-Man in other media TOP-3  Q79037 Spider-Man 
 The crew of Endeavour's final mission, STS-134, which launched on Monday at 8:56 AM EDT.	Q478803 STS-134 25th and last spaceflight of Space Shuttle Endeavour	TOP-1  Q478803 STS-134  TOP-2  Q328927 STS-133 TOP-3  Q460468 STS-132	TOP-1  Q96206891 Endeavour  TOP-2  Q478803 STS-134  TOP-3  Q309080 TS-135	TOP-1  Q1340318 Endeavour  TOP-2  Q182508 Endeavour TOP-3  Q508018 Endeavour

(a) Correct cases.

Input	Ground Truth Entity	VP-MEL (FBMEL)	LLaVA-1.5	MEL (MIMIC)
 2016: that year, US president Donald Trump was named Time "Person of the Year".	Q43297 Time American news magazine and website	TOP-1  Q22686 Donald Trump  TOP-2  Q207826 Time Person of the Year  TOP-3  Q43297 Time 	TOP-1  Q43297 Time  TOP-2  Q22686 Donald Trump  TOP-3  Q207826 Time Person of the Year 	TOP-1  Q207826 Time Person of the Year  TOP-2  Q10714 @ TOP-3  Q23005517 Thank You
 Ozzy and Sharon Osbourne visit the USS Missouri on March 9, 2004.	Q1806985 Sharon Osbourne British-American television personality	TOP-1  Q133151 Ozzy Osbourne  TOP-2  Q1806985 Sharon Osbourne  TOP-3  Q1094412 USS Missouri 	TOP-1  Q133151 Ozzy Osbourne  TOP-2  Q1806985 Sharon Osbourne  TOP-3  Q1094412 USS Missouri 	TOP-1  Q1094412 USS Missouri  TOP-2  Q272560 USS Missouri TOP-3  Q7871862 USS Missouri

(b) Error cases.

Figure 6: Case study for VP-MEL. Each row is a case, which contains Input, ground truth entity, and top three retrieved entities of three methods, i.e., FBMEL (ours), LLaVA-1.5 (Liu et al., 2024), MIMIC (Luo et al., 2023). Each retrieved entity is described by its Wikidata QID and entity name, with the entity marked with a checkmark indicating the correct one.